Mediterranean Archaeology and Archaeometry
Vol. 20, No 3, (2020), pp. 75-89
Open Access. Online & Print.

www.maajournal.com

DOI: 10.5281/zenodo.3930410

INVESTIGATION OF MARBLE DETERIORATION AND DEVELOPMENT OF A CLASSIFICATION SYSTEM FOR CONDITION ASSESSMENT USING NON-DESTRUCTIVE ULTRASONIC TECHNIQUE

Abdelraheem Ahmad

Department of Conservation and Management of Cultural Resources, Faculty of Archaeology and Anthropology, Yarmouk University, Irbid 211-63, Jordan
(abd.ahmad@gmail.com) ORCID: 0000-0001-8840-5050

Received: 18/06/2020
Accepted: 12/07/2020

ABSTRACT

The current paper investigates the influence of artificial thermal weathering on marble for the purpose of developing an improved classification system to assess marble deterioration based on non-destructive ultrasonic velocity measurements. Different samples of historical Greek and Turkish marble used in Roman archaeological structures in two Jordanian archaeological sites were selected and subjected to four heating cycles at different temperatures. The induced changes in the microstructure and physico-mechanical properties of the marble were examined and correlated with ultrasonic wave velocity measurements. Results showed that thermal weathering, particularly at temperatures beyond 200 ˚C, produces considerable microcracking in marble. The developed cracks act to significantly increase the porosity of marble and result in a corresponding significant reduction in ultrasonic velocity of marble. Consequently, a simplified relationship between ultrasonic velocity and marble porosity has been proposed and an improved classification system for assessing marble deterioration has correspondingly been developed. This system allows for efficient assessment of the condition of archaeological marble objects and structures in a simple and non-destructive way. The results of this paper indicate that the deterioration of marble, regardless of its fabric characteristics, can reliably be assessed based on non-destructive ultrasonic velocity measurements. The consideration of rock fabric parameters, however, helps provide a more comprehensive evaluation and interpretation marble damage.

KEYWORDS: Marble, Thermal deterioration, Ultrasonic technique, Weathering classification, Jordan

1. INTRODUCTION

Marble is a prestigious stone that has widely been used since antiquity. An important part of our cultural heritage is built of or carved in marble. Marble is rather a hard rock that is characterized by good physical and mechanical properties, which makes it suitable for construction and sculpturing (Özkan et al., 2013; Siegesmund et al., 2000). Nonetheless, it is subject to deterioration under the action of several agents in the surrounding environment.

The deterioration of marble is related to its composition and microfabric parameters which include microstructure (geometry and morphology of grains and pores) and texture (crystallographic preferred orientation). Marble is mainly composed of calcite crystals which exhibit distinctive thermal anisotropy. Calcite crystals expand when they are heated in the direction parallel to the c-axis, but contracts in the normal directions (Kleber et al., 2010). This anisotropy is considered to be the main factor responsible for marble deterioration, particularly at its early stages (Ruedrich et al., 2010; Sheremeti-Kabashi, 2002; Siegesmund et al., 2000; Zeisig et al., 2002). When marble is subject to temperature changes, thermal stresses are developed that can be sufficiently large to produce microcracks in and between its mineral grains (Battaglia et al., 1993; Robertson, 1982; Weiss, Siegesmund, et al., 2002). The widening of microcracks due to weathering increases the porosity and pore size of marble and changes the water transport mechanism in the stone. This renders the marble more susceptible to damage by other deterioration mechanisms and factors, particularly water (Rüdrich, 2003; Sheremeti-Kabashi, 2002). Consequently, the deterioration rate of marble is considerably accelerated, leading eventually to serious damage or even destruction of marble objects and structures.

Proper conservation of archaeological marble objects and structures requires a detailed assessment of their deterioration level. Traditional methods for condition assessment usually imply taking samples and performing a series of destructive and time-consuming physico-mechanical tests, which is not convenient when dealing with significant stone monuments or objects of arts. As an alternative, non-destructive testing methods have increasingly been developed and applied for investigation of culturally significant materials (Liritzis et al., 2020).

Since the fifties of the last century, non-destructive ultrasonic technique has been widely used for investigating and assessing the condition of stone, particularly marble (Ahmad et al., 2009). This technique is mainly based on propagating ultrasound waves through the stone and measuring their velocity. The velocity of ultrasonic waves depends on the inertial and elastic properties of stone. The latter are greatly influenced by the effects of deterioration such as development of cracks, porosity increase, and decrease in mechanical strength (Gomez et al., 1991). Therefore, correlating changes in stone properties as a result of deterioration with ultrasonic velocity can provide classification systems for evaluating the deterioration level of stone. Köhler (1991) found that the velocity of longitudinal ultrasonic waves in Carrara marble decreases notably upon progressive damage. Accordingly, the author proposed an empirical classification system for marble (Table 1).

Table 1 Classification of marble damage after Köhler (1991)

Ultrasonic pulse velocity (V_p) [km/s]	*Description*	*Damage class*
>4.5	Fresh	I
3–4.5	Increasing porosity	II
2–3	Progressive granular disintegration	III
1–2	Danger of breakdown	IV
<1	Complete structural damage	V

This classification system is based on a correlation between ultrasonic pulse velocity and marble porosity. Modified versions of this system have also been developed and adopted (Akoglu et al., 2019; Simon, 2001). However, many authors argue that an accurate interpretation of the relationship between ultrasonic velocity and stone deterioration level requires comprehensive knowledge of the petrophysical properties of the stone and its fabric (Dürrast et al., 1999; Rüdrich, 2003; Ruedrich et al., 2013; Siegesmund, 1996; Siegesmund et al., 1999, 2007; Weiss et al., 2000). Furthermore, Köhler's classification system was developed for Carrara marble. Carrara marble is a fine-grained marble that has been extensively used in monuments and sculptures since the classical period (Attanasio et al., 2006). However, there are other major sources of historical white marble around the Mediterranean, particularly in Greece and Turkey. In fact, the greater part of marble used in heritage constructions in the eastern and south-eastern Mediterranean region, which is very rich of archaeological sites, originated from different quarries and localities in Turkey and Greece. Some examples of the most important and most widely

used marbles from these locations include the Greek marbles of Penteli, Thasos and Paros and the Turkish marble of Proconnesos (Moropoulou et al., 2019). These marbles were also popular in other parts of the world. Even in Rome, eastern quarries were the major supply sources of architectural marble during the late 2nd century and early 3rd century AD (Attanasio et al., 2006). An updated database of historical white marble quarries used in antiquity can be found in Antonelli & Lazzarini (2015). These historical marble types exhibit a wide range of different characteristics in terms of microfabric, composition and visual properties. Therefore, the characterization and assessment of the deterioration of historical marbles require a comprehensive study on a large variety of samples in order to develop damage classification systems that can be applicable to a wide range of marble types.

In this study, the deterioration of marble as a result of artificial thermal weathering is examined and correlated with ultrasonic wave velocity measurements for a variety of historical marbles widely used in antiquity. This should help us to understand the nature and extent of changes in marble structure and physico-mechanical properties with progressive weathering. The aim of the study is to develop an improved classification system for assessing marble deterioration based on more elaborate correlations between non-destructive ultrasonic velocity and stone properties. Such a system can be applied to assess the condition of archaeological marble, monitor its damage over extended periods of time, and evaluate the effectiveness of applied conservation treatments in a simple, fast and non-destructive way. Compared to earlier relevant studies, this study incorporates a more comprehensive investigation of marble damage using a multidisciplinary approach and a larger variety of historical marbles exhibiting various microstructural characteristics in order to develop an improved classification system for assessing marble condition that can reliably be applied on a wider range of historical marbles.

2. MATERIALS AND METHODS

2.1. Materials

The stone materials investigated in this study consist of six historical marble varieties collected from the archaeological sites of Umm Qais (ancient Gadara) and Jerash (ancient Gerasa) in northern Jordan. They were originally quarried from important historical quarry sources in Greece and Turkey and imported and used in several Roman structures and decorative elements in these two archaeological sites. The studied samples were chosen from a group of marble samples that were already investigated for their characteristics and provenance in a previous study by the author (Ahmad, 2018). Based on the objectives of the study, the stone materials need to be fresh or in sound condition. Therefore, preliminary characterization by macroscopic investigation, ultrasonic velocity measurements and simple physical tests were performed to select only sound, almost unweathered, marble samples for further investigation.

Table 2 The investigated marble samples. He: Heteroblastic; Ho: Homeoblastic; C: Calcite; D: Dolomite; G: Graphite; Q: Quartz (Ahmad, 2018)

Sample	Provenance	Use	Color	Pattern	Mineral comp.	Texture	Microstructure	Crystal boundaries	Maximum grain size [mm]
JM1	Mount Hymettus	Cornice	Light grey	Irregular dark grey streaks	C; D	He/Ho	Mosaic	Curved, embayed	1.12
JM2	Proconnesos	Cornice	Light grey	Irregular dark grey bands	C	He	Mortar	Embayed, sutured	2.5
UM1	Proconnesos	Floor tile	grey	Parallel dark grey lines	C; D; Q	He	Mortar	Curved, sutured	2.64
UM2	Proconnesos	Cornice	grey	Dark grey streaks	C	He	Mortar	Embayed, sutured	2.95
UM3	Proconnesos	Cornice	Light grey	Dark grey bands	C; D	He	Mortar	Curved, Sutured	2.23
UM6	Mount Pentelikon	Column	Light grey	irregular dark grey streak	C; D; Q	He/Ho	Lineated	Curved, embayed	1.4

Table 2 shows the main macroscopic, mineralogical and petrographic characteristics of the studied samples. The samples exhibit different textures, grain sizes and grain boundary shapes. They include

fine-grained marbles that were quarried from Mounts Pentelikon and Hymettus in Greece and medium- to coarse-grained marbles quarried from Proconnesos (Marmara Island) in Turkey. Pentelic marble was widely used during the Hellenistic and Roman periods, particularly in central-eastern Mediterranean and North Africa (Attanasio et al., 2006). It is very famous because of its use for the construction of the Parthenon and many Athenian monuments (Attanasio et al., 2006; Moropoulou et al., 2019). Hymettian marble was commonly used during the Hellenistic and Roman periods; especially in Greece (Cramer, 2004; Herz, 1988). Proconnesos marble is one of the most famous and most widely used marbles in antiquity. It spread all over the Roman Empire and was mainly used for buildings and sarcophagi (Attanasio et al., 2008; Moropoulou et al., 2019).

2.2. *Methods*

2.2.1 Artificial weathering

To study the influence of thermal weathering on marble, dry marble samples were artificially weathered by heating at four different temperatures, namely 100, 200, 300 and 400 °C, for one hour. Heating at high temperatures proved to be an effective method of artificial weathering for calcitic stones (Franzoni et al., 2013). The induced alterations in microstructure and physical and mechanical properties of the heated marble samples were investigated and compared to those of the unheated samples. It is worth mentioning that the measurement of the physical and mechanical properties before artificial thermal weathering requires drying the samples by heating at 60 ˚C to constant mass. According to Siegesmund et al. (2000), the critical temperature at which thermally induced microcracks in marble can be initiated and propagated depends, amongst other, on its grain size and grain boundary shape. For a certain Carrara marble variety, this temperature was found to be around 60-70 ˚C (S. Siegesmund et al., 2000; Siegesmund & Dürrast, 2011). Thermal cracking in marble may nonetheless start at lower temperatures (40-50 ˚C) (Battaglia et al., 1993; Malaga-Starzec et al., 2002; Steiger et al., 2011; Weiss, Siegesmund, et al., 2002; Widhalm et al., 1997). However, it was considered that drying the unweathered samples at this temperature does not cause significant damage and those samples can still be considered intact.

2.2.2. Petrographic and mineralogical analyses

The studied marble samples were already characterized for their petrographic characteristics and mineralogical composition in a previous publication by the author (Ahmad, 2018). This was performed using polarizing light microscope and X-ray diffraction measurements. The changes induced in the microstructure of the samples after heating were investigated on thin sections under Leica polarizing light microscope. Photomicrographs under Cross Polarized Nichols (XPL) were taken by a Leica (ICC 50 HD) camera attached to the microscope.

2.2.3. Physical properties

The physical properties (porosity, density, and capillary water uptake) of the marble samples were determined by water absorption methods on at least 3 cubic specimens of 5 cm side length for each test. The porosity accessible to water (N_t) was measured according to RILEM I.1 (RILEM, 1980). After drying at 60 °C to constant mass (M1), the samples were put in an evacuation vessel under vacuum for 24 hours to eliminate the air contained in the pores. Water was then slowly introduced into the vessel until the samples were completely immersed, and the vacuum was maintained for 24 hours afterwards. The samples were left under water for another 24 hours at atmospheric pressure. Finally, the samples were weighted separately under water (M_2) and directly after removing from water (M3), and the accessible porosity was calculated as follows:

$$N_t = \frac{M_3 - M_1}{M_3 - M_2} \cdot 100 \quad (1)$$

Where N_t= porosity accessible to water [%]; M_1= mass of the dried sample [g]; M_2= mass of the saturated sample under water [g]; M_3= mass of the saturated sample in air [g].

The free porosity (N_{48}) was measured according to RILEM II.1 (RILEM, 1980), by drying the samples to constant mass (M'_1), placing them in a flat container and adding water slowly to allow for capillary water absorption, before immersing them completely in water. After 48 hours of immersion in water, the samples were taken out and weighted (M_{48}). The free porosity was calculated as follows:

$$N_{48} = \frac{M_{48} - M'_1}{M_3 - M_2} \cdot 100 \quad (2)$$

Where N_{48}= free porosity after 48 hours of immersion in water [%]; M_{48}= mass of the sample after 48 hours of immersion in water [g]; M'_1= the mass of the dried sample [g]; M_2= mass of the saturated sample under water [g] as determined above for accessible porosity; M_3= mass of the saturated sample in air [g] as determined above for accessible porosity.

The saturation coefficient (S) was calculated as the ratio of free porosity to accessible porosity. The bulk (ρ_{bulk}) and real (ρ_{real}) densities, which represent the

ratio of the mass to the bulk and impermeable volumes of the stone respectively, were determined according to RILEM I.2 (RILEM, 1980), as follows:

$$\rho_{bulk} = \frac{M_1}{M_3 - M_2} \quad (3)$$

$$\rho_{real} = \frac{M_1}{M_1 - M_2} \quad (4)$$

Where ρ_{bulk}= bulk density [g/cm³]; ρ_{real}= real density [g/cm³].

The capillary water absorption coefficient (w-value) of the stone samples was measured on dry specimens following the standard test DIN EN 1925 (DIN, 1999). The specimens were placed in a flat container and allowed to take water by capillary action. The specimens were weighted in definite time intervals, and the water absorption coefficient was calculated as the slope of the linear part of the curve depicting the amount of absorbed water per area against the square root of time.

$$w = \frac{\Delta m}{A} \cdot \frac{1}{\sqrt{\Delta t}} \quad (5)$$

Where w= water absorption coefficient [kg/(m².h1/2)]; Δm= mass of absorbed water in time interval Δt [kg]; A= the area of the stone surface in contact with water [m²]; Δt = time interval [h].

2.2.4. Uniaxial compressive strength

Uniaxial compressive strength (UCS) was performed on at least 3 cubic specimens of 5 cm side length using DIGITEC Machine equipped with a Universal Testing Machine (UTM II) software. The load was applied on the specimens perpendicular to the foliation plane with a loading rate of 750 N/s until failure. The uniaxial compressive strength was calculated as the maximum load divided by the area of the loaded surface.

2.2.5. Non-destructive ultrasonic velocity measurement

Non-destructive ultrasonic wave velocity measurements were carried out using a Consonic 2-GS ultrasonic measuring device from Geotron-Elektronik with ultrasonic transmitter (UPG) vibrating at 250 kHz and ultrasonic receiver (UPE). The velocity of longitudinal ultrasonic waves transmitted through the stone sample was measured and evaluated using LightHouse software. The coupling between the ultrasonic transducers and the stone was achieved using an acoustic coupling material made of silicone rubber. To take the anisotropy of stone into consideration, the ultrasonic pulse velocity (Vp) was measured along three perpendicular directions. For this purpose, a reference coordinate system (XYZ) with respect to the visible textural elements of foliation and lineation was applied; the z-axis was perpendicular to the foliation plane and the x-axis was along the direction of lineation. At least, three specimens were tested for each stone sample and the average value of at least 3-5 measurements in each direction was calculated. The accuracy of velocity measurement in transmission method is assumed to be ± 50 m/s. Ultrasonic velocity measurements were performed both on dry and water-saturated samples as the velocity of ultrasonic waves in stone is influenced by the degree of water saturation of the pores. These measurements provide useful information about pore space characteristics and density of open cracks in stone. The anisotropy of the stone samples was calculated according to the following equation:

$$A = \frac{V_{P\max} - V_{P\min}}{V_{P\max}} \cdot 100\% \quad (6)$$

Where A= anisotropy [%], V_{Pmax}= the maximum ultrasonic velocity in the three directions [m/s], and V_{Pmin}= the minimum ultrasonic velocity in the three directions [m/s].

3. RESULTS AND DISCUSSIONS

The physical and mechanical properties of the studied marble samples before and after thermal weathering are presented in Table 3.

The accessible porosity of the marble samples increased progressively by 35%, 68%, 203%, and 331% and the free porosity increased by 34%, 75%, 244%, and 404% after heating at 100 ˚C, 200 ˚C, 300 ˚C, and 400 ˚C respectively. This increase of porosity is attributed to the thermally induced cracks between calcite grains. Similarly, the capillary water absorption of the marble samples increased progressively with increasing weathering due to the increase in the proportion of capillary pores and the improved connectivity of pores caused by heating (Ahmad, 2011). The effect of temperature on the physical properties of marble seems to be intensified by heating at temperatures higher than 200 ˚C (Fig. 1). The microscopic investigation of the heated samples confirms this result (Fig. 2). Remarkable changes, represented by development and widening of intergranular and intragranular cracks, in the microstructure of the marble samples heated beyond 200 ˚C have occurred. Below this heating temperature, the induced microstructural changes are relatively small and less significant.

Table 3 The physical and mechanical properties of the marble samples before and after thermal weathering. Temp.: Temperature; N_t: Porosity accessible to water; N_{48}: Free porosity; ρ_{bulk}: Bulk density; ρ_{real}: Real density; S: Saturation coefficient; w-value: Capillary water absorption coefficient; UCS: Uniaxial compressive strength

Sample	Temp.[˚C˙]	N_t[%]	N_{48} [%]	ρ_{real}[g/cm³]	ρ_{bulk}[g/cm³]	S	w-value [kg/(m².h$^{0.5}$)]	UCS [N/mm²]
JM1	Untreated (60)	0.20±0.02	0.13±0.01	2.73±0.01	2.72±0.01	0.66±0.03	0.010±0.000	64.33±3.63
	100	0.29±0.01	0.18±0.00	2.73±0.01	2.72±0.01	0.62±0.01	0.014±0.002	56.58±3.56
	200	0.35±0.01	0.23±0.01	2.72±0.00	2.72±0.00	0.65±0.01	0.024±0.004	44.50±0.67
	300	0.83±0.02	0.67±0.01	2.72±0.00	2.70±0.00	0.80±0.01	0.046±0.003	41.02±0.60
	400	0.99±0.02	0.77±0.03	2.72±0.01	2.69±0.01	0.80±0.01	0.174±0.011	33.87±1.10
JM2	Untreated (60)	0.24±0.03	0.15±0.02	2.72±0.00	2.71±0.00	0.57±0.06	0.014±0.005	54.13±6.63
	100	0.35±0.02	0.24±0.01	2.72±.00	2.71±0.00	069±0.01	0.020±0.001	48.78±4.56
	200	0.40±0.03	0.26±0.03	2.72±0.00	2.71±0.00	0.65±0.01	0.038±0.006	40.11±3.96
	300	0.62±0.02	0.45±0.04	2.72±0.00	2.70±0.00	0.72±0.04	0.124±0.004	37.44±3.81
	400	0.99±0.02	0.77±0.03	2.72±0.01	2.69±0.01	0.78±0.02	0.347±0.064	30.34±2.91
UM1	Untreated (60)	0.23±0.02	0.18±0.02	2.72±0.00	2.72±0.00	0.79±0.06	0.041±0.005	81.19±5.43
	100	0.34±0.01	0.22±0.00	2.72±0.00	2.71±0.00	0.64±0.02	0.098±0.005	80.24±1.18
	200	0.46±0.02	0.37±0.00	2.72±0.00	2.71±0.00	0.79±0.04	0.156±0.005	66.86±8.84
	300	0.83±0.01	0.65±0.02	2.72±0.00	2.70±0.00	0.78±0.03	0.414±0.021	64.86±0.51
	400	1.18±0.03	0.99±0.03	2.72±0.00	2.69±0.00	0.84±0.02	0.525±0.012	58.32±5.06
UM2	Untreated (60)	0.44±0.00	0.30±0.00	2.72±0.00	2.71±0.00	0.68±0.01	0.094±0.000	48.69±2.81
	100	0.45±0.01	0.32±0.00	2.72±0.00	2.71±0.00	0.71±0.01	0.106±0.013	41.50±1.90
	200	0.60±0.02	0.46±0.01	2.72±0.00	2.70±0.00	0.77±0.01	0.166±0.004	36.80±6.70
	300	0.97±0.00	0.83±0.02	2.72±0.00	2.69±0.00	0.85±0.01	0.448±0.022	30.33±0.32
	400	1.39±0.01	1.21±0.01	2.72±0.00	2.68±0.00	0.88±0.00	0.551±0.049	28.92±0.71
UM3	Untreated (60)	0.23±0.01	0.18±0.01	2.72±0.00	2.71±0.00	0.80±0.07	0.008±0.001	57.51±1.29
	100	0.34±0.01	0.25±0.00	2.72±0.00	2.71±0.00	0.74±0.01	0.012±0.002	47.69±2.16
	200	0.40±0.02	0.32±0.01	2.72±0.00	2.71±0.00	0.80±0.02	0.029±0.002	36.54±0.78
	300	0.81±0.03	0.66±0.02	2.72±0.00	2.70±0.00	0.84±0.00	0.079±0.004	31.10±3.00
	400	1.17±0.10	0.99±0.11	2.72±0.00	2.69±0.00	0.84±0.03	0.328±0.079	24.64±1.46
UM6	Untreated (60)	0.39±0.03	0.35±0.02	2.73±0.00	2.71±0.00	0.90±0.04	0.053±0.002	46.35±2.20
	100	0.46±0.03	0.42±0.03	2.72±0.00	2.71±0.00	0.92±0.05	0.095±0.001	41.91±1.59
	200	0.56±0.02	0.50±0.03	2.72±0.00	2.70±0.00	0.89±0.02	0.154±0.003	31.24±0.99
	300	0.75±0.01	0.71±0.02	2.71±0.00	2.69±0.00	0.95±0.01	0.420±0.006	23.57±1.30
	400	1.29±0.06	1.25±0.03	2.71±0.00	2.68±0.00	0.97±0.02	0.891±0.007	18.78±0.75

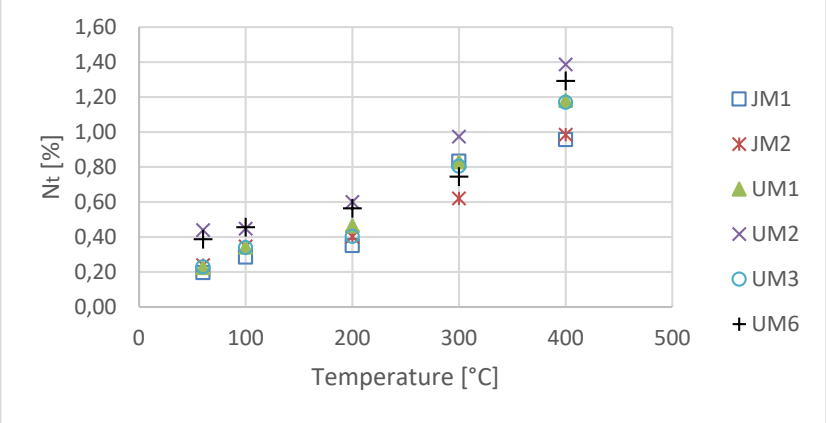

Fig. 1. The accessible porosity of the marble samples at different temperature.

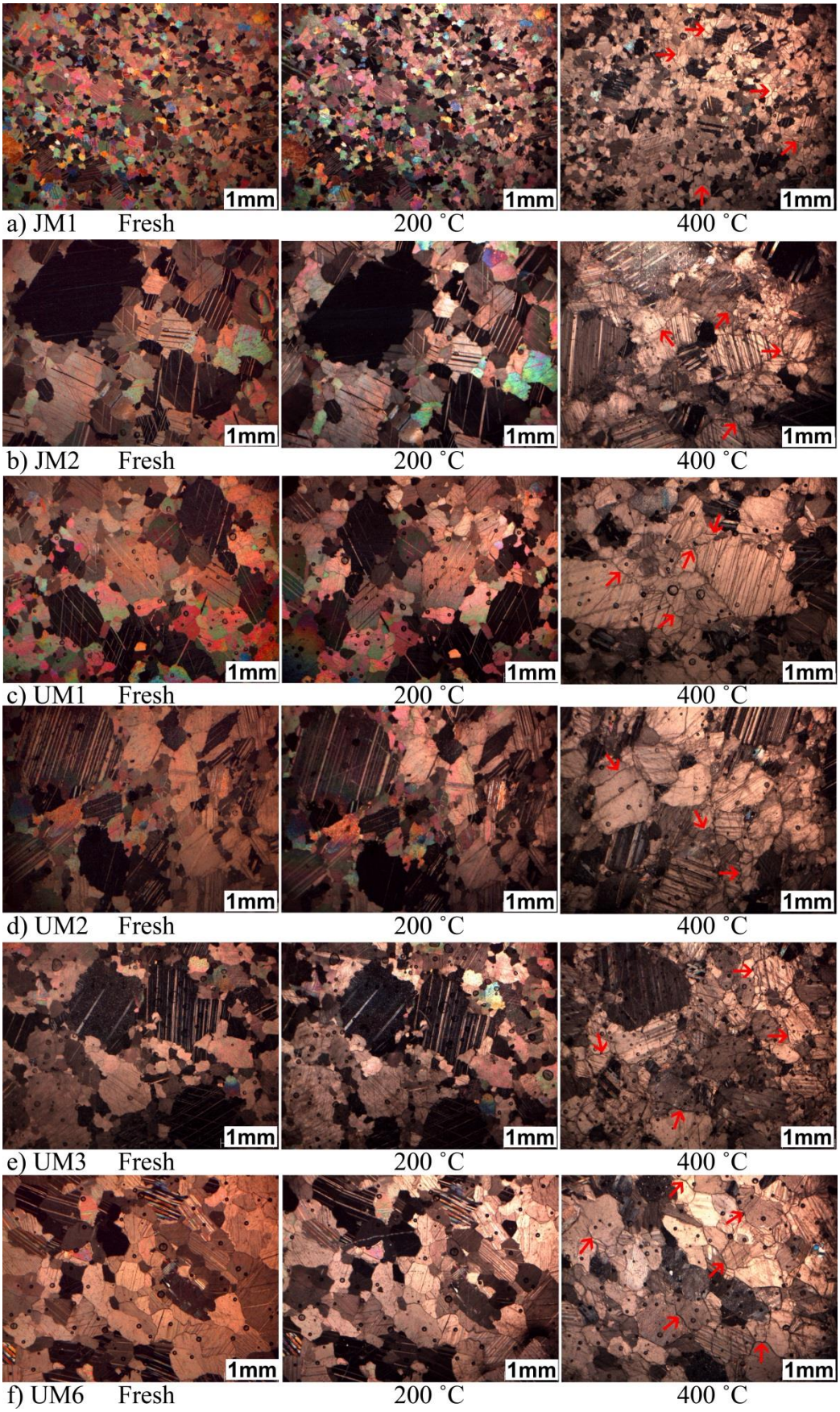

Fig. 2. Photomicrographs of thin sections of the fresh marbles and heated samples at 200 ˚C and 400˚C. The red arrows indicate thermally induced microcracks in and between calcite crystals. The photomicrographs of the fresh marble samples are already published in a previous publication by the author (Ahmad, 2018).

The mechanical strength of the marble samples was also affected by thermal weathering. An average decrease in uniaxial compressive strength of about 11%, 28%, 37% and 46% was recorded after heating at 100 ˚C, 200 ˚C, 300 ˚C, and 400 ˚C respectively. The decrease in mechanical strength with increasing weathering can be attributed to the development of microcracks, which weaken grain cohesion and stone structure (Ahmad, 2011).

The results of ultrasonic velocity measurements on the studied marble samples before and after thermal weathering are summarized in Table 4. For most of the samples, the anisotropy of ultrasonic velocity in dry condition shows an increasing trend with increasing weathering. This might indicate a directional dependence of thermal cracking; a greater propagation of thermally induced cracks in the direction perpendicular to the z-axis (i.e. parallel to the foliation plane). However, the anisotropy of sample UM3 decreased with increasing thermal weathering. The anisotropy of ultrasonic velocity is lower in water-saturated condition than in dry condition for all the samples. This can be attributed to the mitigation of cracks influence by water.

Table 4 Ultrasonic velocity in dry and water-saturated conditions before and after thermal weathering

Sample	Temp. [˚C]	Dry condition			A Dry	Water-saturated condition			A Saturated	ΔV (Saturated-Dry)			Avg. ΔV% [%]
		Vp_x [m/s]	Vp_y [m/s]	Vp_z [m/s]		Vp_x [m/s]	Vp_y [m/s]	Vp_z [m/s]		Vp_x [m/s]	Vp_y [m/s]	Vp_z [m/s]	
JM1	UT	5875	5588	5501	6.34	5945	5719	5614	5.54	71	132	112	2
	100	4226	4166	4192	1.44	5431	5431	5415	0.30	1205	1266	1223	29
	200	4241	4075	3871	8.74	5404	5048	4999	7.51	1163	973	1128	27
	300	3052	2870	2725	10.71	4242	4178	4048	4.57	1190	1307	1323	44
	400	3067	2482	2481	19.12	4419	4110	4024	8.94	1351	1628	1543	57
JM2	UT	5770	5555	5372	6.90	5921	5708	5625	5.01	151	153	254	3
	100	4420	4274	4164	5.79	5695	5587	5454	4.23	1275	1313	1290	30
	200	4068	3894	3585	11.88	5253	5226	4967	5.44	1185	1332	1383	34
	300	3370	3202	2977	11.64	4778	4575	4434	7.19	1408	1373	1457	45
	400	2788	2658	2458	11.82	4520	4486	4353	3.65	1732	1829	1895	69
UM1	UT	5996	5453	4808	19.79	6108	5770	5299	13.21	112	317	491	6
	100	4936	4438	3924	20.46	5616	5516	5224	6.92	680	1078	1299	24
	200	3907	3382	3228	17.16	5056	4595	4542	10.15	1149	1213	1314	35
	300	3619	2943	2569	29.04	5015	4759	4452	11.22	1396	1816	1884	58
	400	3011	2447	2170	27.54	4679	4572	4405	5.81	1668	2126	2234	82
UM2	UT	4252	4040	3311	22.18	5354	5267	4819	9.98	1102	1227	1508	34
	100	3759	3581	3398	9.61	5236	5084	4810	8.15	1477	1503	1412	41
	200	3040	2901	2561	15.77	4041	3933	3759	6.98	1001	1032	1198	38
	300	2640	2573	2170	17.79	3622	3516	3197	11.75	982	943	1026	40
	400	2492	2336	1918	23.03	3563	3484	3546	0.48	1071	1148	1628	59
UM3	UT	5956	5761	5310	10.84	6010	5767	5422	9.79	54	6	112	1
	100	5009	4611	4300	14.16	5199	5192	4708	9.44	190	581	409	9
	200	4149	3751	3568	13.99	4893	4878	4579	6.41	744	1127	1011	25
	300	3153	2857	2880	8.65	4504	4419	4369	3.00	1351	1562	1488	50
	400	2440	2286	2282	6.55	4133	3946	3891	5.86	1693	1660	1609	71
UM6	UT	4501	4039	3922	12.88	4763	4530	4463	6.31	262	491	541	11
	100	4058	3652	3528	13.08	4261	4047	3957	7.13	203	395	429	9
	200	3402	3007	2908	14.47	3903	3576	3473	11.02	501	569	565	18
	300	2771	2584	2401	13.36	3359	3139	2978	11.44	588	555	577	22
	400	2302	2004	1951	15.25	3047	2790	2651	13.16	745	786	700	36

The ultrasonic velocity of the untreated samples in water-saturated condition showed a small increase by 2%, 3%, 6%, 1% and 9% compared to dry condition for the samples JM1, JM2, UM1, UM3, and UM6 respectively. The increase of ultrasonic velocity in water-saturated condition can be explained by the presence of some pre-existing cracks in the fresh marble samples. The presence of such cracks in fresh crystalline rocks is usually expected (Siegesmund et al., 2000). Sample UM2 showed, however, a greater proportion of pre-existing cracks in the untreated condition, as indicated by the greater variation (34%) in ultrasonic velocity between dry and water-saturated specimens. This sample exhibited already a higher level of deterioration and it is actually not that fresh.

The variation in ultrasonic velocity between dry and water-saturated condition increased significantly with increasing thermal weathering to 57%, 69%, 82%, 59%, 71% and 36% for the samples JM1, JM2, UM1, UM2, UM3 and UM6 respectively at the end of the test. This can be attributed to the development of microcracks with increasing thermal weathering. Microcracks act to significantly decrease the ultrasonic velocity in dry samples, whereas their influence on ultrasonic velocity in water-saturated samples seems to be mitigated by the crack-bridging caused by water (Ahmad, 2011; Rodrigues, 1982).

On examining possible correlations between marble properties upon weathering, strong correlation could be found between accessible porosity and the velocity of ultrasonic longitudinal waves in the dry marble samples (Fig. 3). The functional relationship between ultrasonic velocity and accessible porosity takes the form of a power function ($Vp=2.5243x(N_t)^{-0.495}$). For simplicity, this correlation could be approximated, and the following equation can, thus, be proposed for the relationship between ultrasonic velocity and accessible porosity.

$$V_P = \frac{2.5}{\sqrt{N_t}} \quad (7)$$

Where V_P= Ultrasonic velocity in dry marble [Km/s] and N_t= Accessible porosity [%].

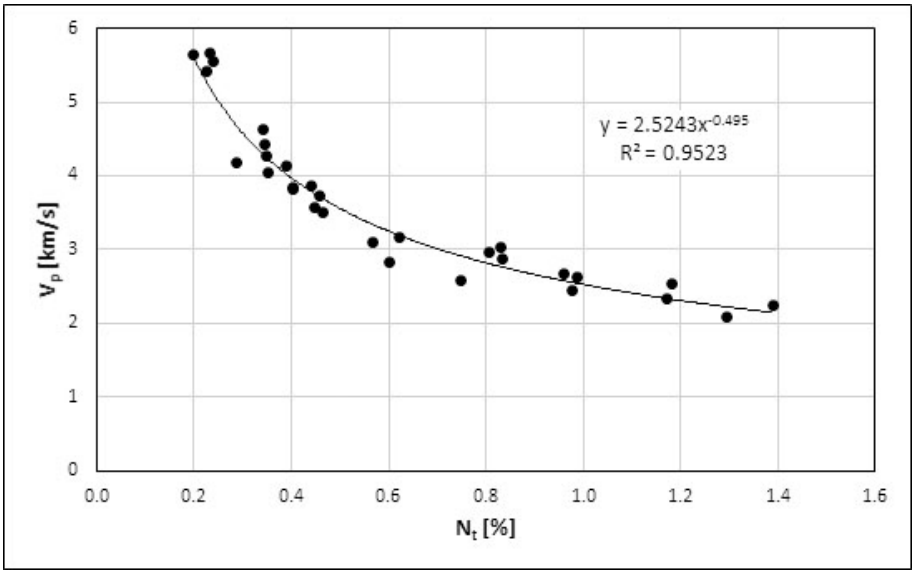

Fig. 3. The relationship between ultrasonic pulse velocity and accessible porosity.

This relationship is almost similar to that developed by Köhler (1991) ($V_p = \sqrt{12/porosity}$). However, it seems to fit the obtained results much better as shown in Fig. 4, which plots the measured results, the proposed correlation and Köhler's correlation.

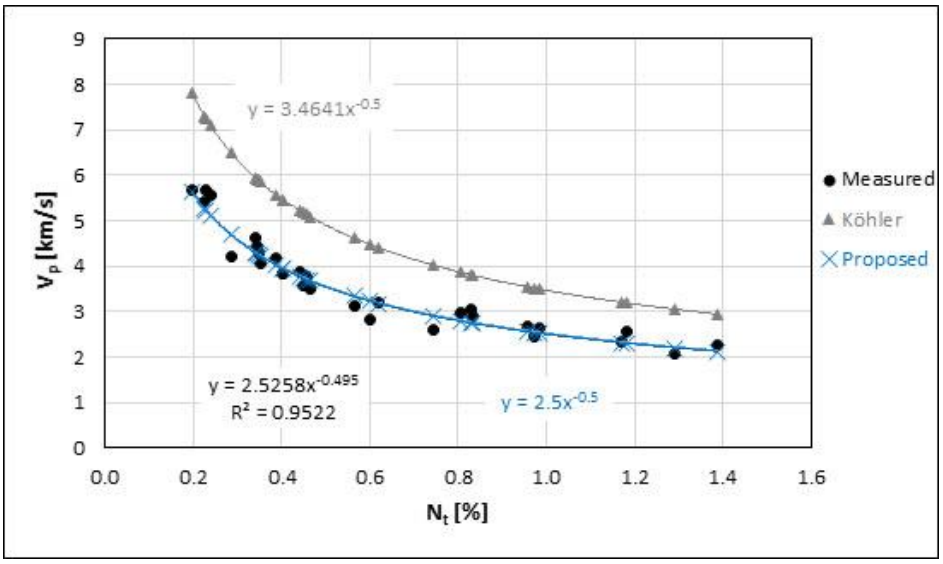

Fig. 4. The measured results, the proposed correlation, and that of Köhler as a function of accessible porosity.

The validity of the proposed relationship was assessed using experimental data from relevant literature. Fig. 5 shows a comparison between the proposed relationship and Köhler's correlation against experimental data from several literature sources (Luque et al., 2011; Martínez-Martínez et al., 2011; Murru et al., 2018; Ruedrich et al., 2013; Sassoni & Franzoni, 2014; Sheremeti-Kabashi, 2002; Ugur et al., 2014; Weiss et al., 2000; Yavuz et al., 2010). It can be seen that the proposed relationship is in good agreement with experimental data, particularly for weathered marble with porosity higher than 1%, and it fits them better than that of Köhler (1991). The small discrepancy found between calculated and experimental data for marble with lower porosity could be attributed to differences in the experimental procedures and testing methods used to obtain the data. For example, the porosity value of stone measured by mercury intrusion porosimetry (MIP) technique may considerably be different from that measured by water absorption method (Cnudde et al., 2009; Hall & Hamilton, 2016). Sheremeti-Kabashi (2002) reported differences up to 140% between the results of marble porosity obtained by these two methods, and attributed this variation to the smaller sample size required for MIP technique, which cannot be sufficient to represent the local inhomogeneity of marble. Consequently, such discrepancy can be expected, particularly for very low porosity marble where small changes in porosity might correspond to significant changes in microstructure and measured ultrasonic velocity. This effect can clearly be seen in the experimental data from Sassoni & Franzoni (2014) and Murru et al. (2018), where the porosity of Carrara marble measured by MIP technique were seemingly overestimated. Since the relationship between ultrasonic velocity and porosity takes the form of an inverse power function, the variation between predicted and experimental data will be greater for the lower values of porosity. Therefore, the experimental values of the unweathered less porous marble are shifted further right from their predicted positions in Fig. 5, whereas the shift was less significant for the larger porosity values of the thermally weathered marble, which almost coincide with the predicted curve.

The data from Sheremeti-Kabashi (2002) have also contributed to the reported discrepancy in the range of low porosity values. This study followed a standard test method for measuring porosity that requires drying the samples before measurement at 105±5 °C, which is clearly higher than the aforementioned critical crack initiation temperatures for marble and could therefore be responsible for the larger porosity values measured in untreated marble samples. Furthermore, the used literature data were almost obtained for Carrara marble and other marble types that mostly do not belong to important historical marbles widely used in antiquity (see Antonelli & Lazzarini (2015)). Unfortunately, there is only limited published literature that contains both porosity and ultrasonic velocity data for important historical marbles used in antiquity, other than Carrara. Further experimental research on this topic is therefore recommended. Notwithstanding all these limitations, the calculated results are generally in good agreement with experimental data, which confirms the validity of the proposed relationship.

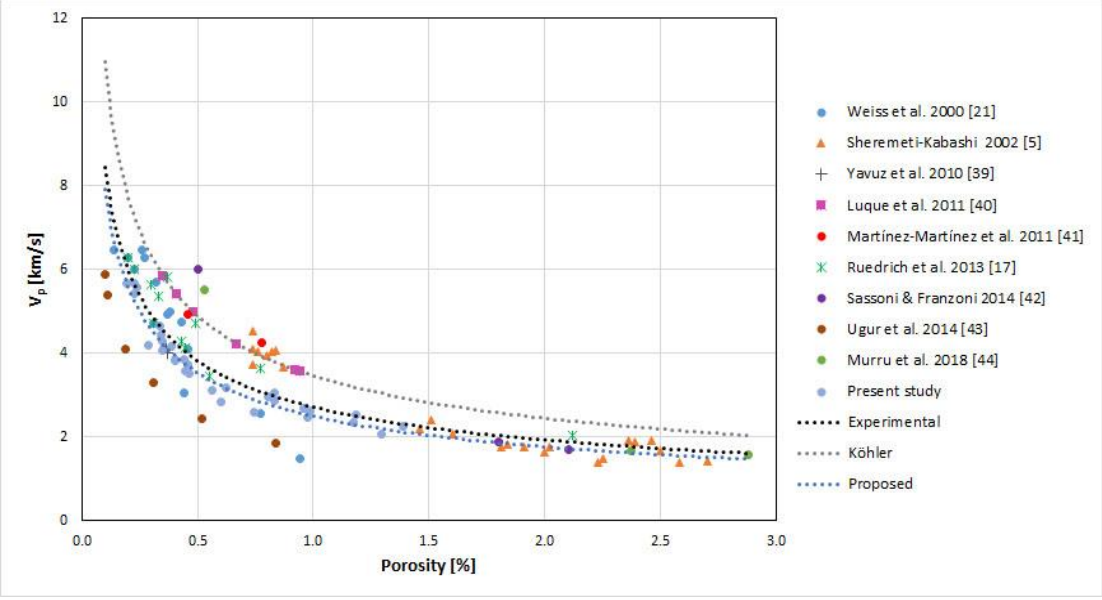

Fig. 5. Comparison of the proposed relationship and Köhler's correlation against experimental data from the literature.

Based on this proposed relationship between ultrasonic velocity and accessible porosity, the following classification system (Table 5) can be developed to evaluate the deterioration level of marble. The description of the deterioration state was given based on visual inspection and examination of the physical and mechanical properties of the marble samples. Similar terms to those adopted in previous publications (Akoglu et al., 2019; Köhler, 1991; Simon, 2001) were used to describe the deterioration state of marble.

Table 5 The proposed classification system for assessing marble condition

Vp [Km/s]	N_t [%]	Damage Class	Color	Description
> 5.0	< 0.25	1	Green	Sound - unweathered
3.5– 5.0	0.25 – 0.5	2	Cyan	Increasing porosity
2.5 – 3.5	0.5 – 1.0	3	Yellow	Granular disintegration
1.5 –2.5	1.0 – 3.0	4	Magenta	Danger of breakdown
< 1.5	> 3.0	5	Red	Complete structural damage

The classification system developed here is not far from that developed by Köhler (1991), but it provides a better approximation to measured velocities. It can be considered as an improved form of Köhler's system, at least for the studied marble varieties and those sharing similar characteristics. The obtained results confirm that marble deterioration can effectively be assessed using the ultrasonic velocity and porosity correlation alone. This result seems to contradict earlier findings (Rüdrich, 2003; Ruedrich et al., 2013; Siegesmund, 1996; Siegesmund et al., 1999; Weiss et al., 2001, 2000), which emphasize the importance of rock fabric parameters in the characterization of marble damage and doubt the reliability of damage assessment based only on correlations between ultrasonic velocity and porosity of marble. According to Weiss et al. (2000), the reduction in ultrasonic velocity with increasing weathering can be related to the geometry of induced cracks defined by crack thickness or aspect ratio (ratio of the small axis to the large axis of the ellipsoidal crack). Model calculations based on the theoretical approach of O'Connell & Budiansky (1974) revealed that ultrasonic velocity can strongly be decreased with only a small increase of marble porosity when the induced cracks are very thin; having an aspect ratio of about 0.005 (Weiss et al., 2000). However, Shearer (1988) showed that the reduction in ultrasonic pulse velocity of rocks is less important for thin cracks with aspect ratios below 0.005. Furthermore, Ruedrich et al. (2013) believe that this hypothetical model applies for marble with purely mechanical crack formation. They pointed out that marbles with crack geometry in form of pitting corrosion may follow the empirical velocity-porosity relationship developed by Köhler (1991). These authors attributed the decrease in velocity with increasing weathering of marble to the progressive increase in density and width of cracks, without ignoring the importance of crack type and distribution, which can be correlated to certain fabric parameters and grain shape fabric (Ruedrich et al., 2013).

It is true that the composition and rock fabric parameters influence the tendency of marble to microcracking and its deterioration in terms of direction and magnitude (Shushakova et al., 2013; Siegesmund et al., 2000; Weiss, Rasolofosaon, et al., 2002). Nonetheless, good evaluation of marble damage can still be achieved using only the velocity-porosity correlation. The development and expansion of microcracks with progressive weathering act to increase the porosity of marble. This increase of porosity seems to cause a corresponding decrease in ultrasonic velocity. Consequently, the deterioration level of marble, regardless of its fabric parameters, can reliably be evaluated based only on the relationship between ultrasonic velocity and porosity of marble as proved empirically in this study. The consideration of rock fabric parameters helps provide a more comprehensive characterization and interpretation of marble damage; but failing to consider them seems not to ruin the sufficiency of the velocity-porosity correlation for assessing marble condition as has been debated.

It should be noted that the classification system proposed here is developed based on ultrasonic velocity measurements on dry marble samples. Therefore, it is important to consider the drying state when applying this system to evaluate the damage of marble objects. Water present in the pore space of marble can significantly affect the velocity of ultrasonic velocity and may thus lead to misleading evaluation of marble deterioration. This fact has already been highlighted in many previous studies (e.g.: Ahmad et al. (2009) and Ruedrich et al. (2013)).

4. CONCLUSIONS

This paper has investigated the deterioration of marble as a result of artificial thermal weathering for the aim of developing an improved classification system for assessing marble deterioration based on non-destructive ultrasonic velocity measurements. Historical marble samples from Jordan were selected and subjected to four heating cycles at different temperatures. The induced changes in the microstructure and physico-mechanical properties of the marble were examined and correlated with ultrasonic wave velocity measurements.

The physical and mechanical properties of the marble samples were significantly influenced by progressive thermal weathering due to the development and expansion of microcracks. However, the effect of thermal weathering seems to be particularly greater on the marble samples heated at temperatures higher than 200 ˚C as confirmed by microscopic investigation on thin sections.

Most of the studied marbles showed directional dependence of thermal cracking as indicated by the increase of the anisotropy of ultrasonic velocity in dry samples with increasing thermal weathering. The decrease in ultrasonic velocity with increasing thermal weathering is clearly evident for dry marble samples compared to water-saturated ones. The effect of thermally induced microcracks on ultrasonic velocity of water-saturated samples seems to be mitigated by water.

Strong correlation has been found between the velocity of ultrasonic longitudinal waves in dry condition and porosity of marble. The validity of the proposed correlation has been confirmed using experimental data from the literature. Consequently, a classification system for assessing the deterioration level of marble by ultrasonic velocity measurements has been developed. This allows for conducting efficient assessment of marble deterioration in a simple and non-destructive way. The proposed correlation and classification system provide a better approximation to measured values than previously developed ones. However, it should be noted that the classification system is developed using ultrasonic velocity measurements on dry marble samples. It is, therefore, necessary to consider the drying state of marble when applying this system. Disregarding the drying state of marble may lead to inaccurate assessment of its condition.

In general, the results of this study provide additional support for the idea that a reliable evaluation of marble deterioration can be achieved based only on a porosity–velocity correlation. Failing to consider the fabric parameters of marble seems not to ruin the validity of this correlation to provide reliable assessment of marble deterioration as has been debated. However, one should not underestimate the importance of rock fabric parameters, which are helpful for providing a more comprehensive characterization and interpretation of marble damage. Further research using a wider marble variety and a greater number of samples is recommended to validate the findings of this study.

ACKNOWLEDGEMENTS

This research was supported by a grant of the Deanship of Research and Graduate Studies at Yarmouk University, Jordan. The author would like to thank the Department of Antiquities of Jordan (DoA) for the permission to collect and study the samples.

REFERENCES

Ahmad, A. (2011). *Characterization of natural and consolidated stones from Jordan with non-destructive ultrasonic technique and physico-mechanical methods*. Technische Universität Dortmund.

Ahmad, A. (2018). Archaeometric and provenance study of archaeological marble from Gadara and Gerasa in Jordan. *Applied Physics A*, *124*, 514. https://doi.org/10.1007/s00339-018-1940-7

Ahmad, A., Pamplona, M., & Simon, S. (2009). Ultrasonic testing for the investigation and characterization of stone – a non-destructive and transportable tool. *Studies in Conservation, 54, 43–53. https://doi.org/10.1179/sic2009.54.Supplement-1.43*

Akoglu, K. G., Kotoula, E., & Simon, S. (2019). Combined use of ultrasonic pulse velocity (UPV) testing and digital technologies: A model for long-term condition monitoring memorials in historic Grove Street Cemetery, New Haven. *Journal of Cultural Heritage*, *xxx*, xxx–xxx. https://doi.org/10.1016/j.culher.2019.07.015

Antonelli, F., & Lazzarini, L. (2015). An updated petrographic and isotopic reference database for white marbles used in antiquity. *Rendiconti Lincei*, *26*(4), 399–413. https://doi.org/10.1007/s12210-015-0423-4

Attanasio, D., Brilli, M., & Bruno, M. (2008). The properties and identification of marble from proconnesos (Marmara Island, Turkey): A new database including isotopic, EPR and petrographic data. *Archaeometry*, *50*(5), 747–774. https://doi.org/10.1111/j.1475-4754.2007.00364.x

Attanasio, D., Brilli, M., & Ogle, N. (2006). *The isotopic signature of classical marbles*. L'Erma di Bretschneider.

Battaglia, S., Franzini, M., & Mango, F. (1993). High-sensitivity apparatus for measuring linear thermal expansion: Preliminary results on the response of marbles to thermal cycles. *Il Nuovo Cimento*, *16*(4), 453–461. https://doi.org/10.1007/BF02507653

Cnudde, V., Cwirzen, A., Masschaele, B., & Jacobs, P. J. S. (2009). Porosity and microstructure characterization of building stones and concretes. *Engineering Geology*, *103*(3–4), 76–83. https://doi.org/10.1016/j.enggeo.2008.06.014

Cramer, T. (2004). *Multivariate Herkunftsanalyse von Marmor auf petrographischer und geochemischer Basis*. Technische Universität Berlin.

DIN Deutsches Institut für Normung. (1999). *DIN EN 1925: Prüfverfahren von Naturstein - Bestimmung des Wasseraufnahmekoeffizienten infolge Kapillarwirkung*.

Dürrast, H., Siegesmund, S., & Prasad, M. (1999). Die Schadensanalyse von Naturwerksteinen mittels Ultraschalldiagnostik: Möglichkeiten und Grenzen. *Zeitschrift Der Deutschen Geologischen Gesellschaft*, *150*(2), 359–374. http://www.schweizerbart.de//papers/zdgg_alt/detail/150/55279/Die_Schadensanalyse_von_Naturwerksteinen_mittels_Ultraschalldiagnostik_Moglichkeiten_und_Grenzen

Franzoni, E., Sassoni, E., Scherer, G. W., & Naidu, S. (2013). Artificial weathering of stone by heating. *Journal of Cultural Heritage*, *14*(3 SUPPL), e85–e93. https://doi.org/10.1016/j.culher.2012.11.026

Gomez, M., Cardu, M., & Mancini, R. (1991). Nondestructive testing for soundness of stone architectural pieces. In N. S. Baer, C. Sabbioni, & A. I. Sors (Eds.), *Science, Technology and European Cultural Heritage* (pp. 583–586). Butterworth-Heinemann. https://doi.org/10.1016/B978-0-7506-0237-2.50095-2

Hall, C., & Hamilton, A. (2016). Porosities of building limestones: using the solid density to assess data quality. *Materials and Structures/Materiaux et Constructions*, *49*(10), 3969–3979. https://doi.org/10.1617/s11527-015-0767-3

Herz, N. (1988). The oxygen and carbon isotopic data base for classical marble. In *Classical Marble: Geochemistry, Technology, Trade* (Herz, Norm, pp. 305–314). Kluwer Academic Publishers.

Kleber, W., Bautsch, H.-J., Bohm, J., & Klimm, D. (2010). *Einführung in die Kristallographie*. De Gruyter. https://doi.org/10.1515/9783486598858

Köhler, W. (1991). Untersuchungen zu Verwitterungsvorga¨ngen an Carrara-Marmor in Potsdam Sanssouci. In *Berichte zu Forschung und Praxis der Denkmalpflege in Deutschland, Steinscha¨den – Steinkonservierung* (pp. 50–54).

Liritzis, I., Laskaris, N., Vafiadou, A., Karapanagiotis, I., Volonakis, P., Papageorgopoulou, C., & Bratitsi, M. (2020). Archaeometry: an overview. *Scientific Culture*, *6*(1), 49–98. https://doi.org/10.5281/zenodo.3625220

Luque, A., Ruiz-Agudo, E., Cultrone, G., Sebastián, E., & Siegesmund, S. (2011). Direct observation of microcrack development in marble caused by thermal weathering. *Environmental Earth Sciences*, *62*(7), 1375–1386. https://doi.org/10.1007/s12665-010-0624-1

Malaga-Starzec, K., Lindqvist, J. E., & Schouenborg, B. (2002). Experimental study on the variation in porosity of marble as a function of temperature. *Geological Society Special Publication*, *205*, 81–88. https://doi.org/10.1144/GSL.SP.2002.205.01.07

Martínez-Martínez, J., Benavente, D., & García-del-Cura, M. A. (2011). Spatial attenuation: The most sensitive ultrasonic parameter for detecting petrographic features and decay processes in carbonate rocks. *Engineering Geology*, *119*(3–4), 84–95. https://doi.org/10.1016/j.enggeo.2011.02.002

Moropoulou, A., Delegou, E. T., Apostolopoulou, M., Kolaiti, A., Papatrechas, C., Economou, G., & Mavrogonatos, C. (2019). The white marbles of the Tomb of Christ in Jerusalem: Characterization and provenance. *Sustainability*, *11*(9), 1–35. https://doi.org/10.3390/su11092495

Murru, A., Freire-Lista, D. M., Fort, R., Varas-Muriel, M. J., & Meloni, P. (2018). Evaluation of post-thermal shock effects in Carrara marble and Santa Caterina di Pittinuri limestone. *Construction and Building Materials*, *186*, 1200–1211. https://doi.org/10.1016/j.conbuildmat.2018.08.034

O'Connell, R. J., & Budiansky, B. (1974). Seismic velocities in dry and saturated cracked solids. *Journal of Geophysical Research*, *79*(35), 5412–5426.

Özkan, V., Sarpun, I. H., & Tuncel, S. (2013). *Relative Effects of Porosity and Grain Size on Ultrasonic Wave Propagation in Marbles*.

RILEM TC 25-PEM. (1980). Recommended tests to measure the deterioration of stone and to assess the effectiveness of treatment methods. *Materials and Structures*, *13*(75), 175–253.

Robertson, E. C. (1982). Physical Properties of Building Stone. In *Conservation of Historic Stone Buildings and*

Monuments (pp. 62–86). National Academies Press. https://doi.org/10.17226/514

Rodrigues, J. D. (1982). Laboratory study of thermally fissured rocks. *Fourth International Congress on the Deterioration and Preservation of Stone Objects*, 281–294.

Rüdrich, J. M. (2003). *Gefügekontrollierte Verwitterung natürlicher und konservierter Marmore*. Georg-August-Universität zu Göttingen.

Ruedrich, J., Knell, C., Enseleit, J., Rieffel, Y., & Siegesmund, S. (2013). Stability assessment of marble statuaries of the Schlossbru (Berlin , Germany) based on rock strength measurements and ultrasonic wave velocities. *Environ Earth Sci*, *69*, 1451–1469. https://doi.org/10.1007/s12665-013-2246-x

Ruedrich, J., Rieffel, Y., Pirskawetz, S., Alpermann, H., Joksch, U., Gengnagel, C., Weise, F., Plagge, R., Jianhua Zhao, & Siegesmund, S. (2010). Development and assessment of protective winter covers for marble statuaries of the Schlossbru¨cke, Berlin (Germany). *Environ Earth Sci*. https://doi.org/10.1007/s12665-010-0765-2

Sassoni, E., & Franzoni, E. (2014). Influence of porosity on artificial deterioration of marble and limestone by heating. *Applied Physics A: Materials Science and Processing*, *115*(3), 809–816. https://doi.org/10.1007/s00339-013-7863-4

Shearer, P. M. (1988). Cracked media , Poisson's ratio and the structure of the upper oceanic crust. *Geophysical Journal*, *92*, 357–362.

Sheremeti-Kabashi, F. (2002). *Untersuchungen der Gefügeanisotropie von Carrara-Marmor und deren Einfluss auf die Verwitterung* (Issue April). Ludwig-Maximilians-Universität München.

Shushakova, V., Fuller Jr., E. R., Heidelbach, F., Mainprice, D., & Siegesmund, S. (2013). Marble decay induced by thermal strains: simulations and experiments. *Environ Earth Sci*, *69*, 1281–1297. https://doi.org/10.1007/s12665-013-2406-z

Siegesmund, S., Weiss, T., & Tschegg, E. K. (2000). Control of marble weathering by thermal expansion and rock fabrics. *Proceedings of the 9th International Congress on Deterioration and Conservation of Stone*, 205–213. https://doi.org/10.1016/b978-044450517-0/50102-1

Siegesmund, Siegfried. (1996). The Significance of rock fabrics for the geological interpretation of geophysical anisotropies. In *Geotektonische Forschungen* (85th ed., pp. 1–123). Schweizerbart Science Publishers. http://www.schweizerbart.de//publications/detail/isbn/9783510500512/Geotekt_Forsch_H_85

Siegesmund, Siegfried, & Dürrast, H. (2011). Physical and mechanical properties of rocks. In Siegfried Siegesmund & R. Snethlage (Eds.), *Stone in Architecture: Properties, Durability* (4th ed., pp. 97–225). Springer. https://doi.org/DOI 10.1007/978-3-642-14475-2_3

Siegesmund, Siegfried, Koch, A., & Ruedrich, J. (2007). Ursachen mangelnder Formbeständigkeit von Fassadenplatten: Fallstudie Universitätsbibliothek der Universität Göttingen. *Rohstoff Naturstein Teil*, *1*, 630–648.

Siegesmund, Siegfried, Ullemeyer, K., Weiss, T., & Tschegg, E. . K. (2000). Physical weathering of marbles caused by anisotropic thermal expansion. *Int J Earth Sci*, *89*(1), 170–182. https://doi.org/10.1007/s005310050324

Siegesmund, Siegfried, Weiss, T., Vollbrecht, A., & Ullemeyer, K. (1999). Marble as a natural building stone: rock fabrics, physical and mechanical properties. *Zeitschrift Der Deutschen Geologischen Gesellschaft*, *150*(2), 237–257. http://www.schweizerbart.de//papers/zdgg_alt/detail/150/55272/Marble_as_a_natural_building_stone_rock_fabrics_physical_and_mechanical_properties

Simon, S. (2001). *Zur Verwitterung und Konservierung Kristallinen Marmors Untersuchungen zu physiko-mechanischen Gesteinskennwerten, zur Oberflächenchemie von Calcit und zur Anpassung und Überprüfung von Gesteinsschutzmitteln*. Ludwig-Maximilians-Universität München.

Steiger, M., Charola, A. E., & Sterflinger, K. (2011). Weathering and deterioration. In Siegfried Siegesmund & R. Snethlage (Eds.), *Stone in Architecture: Properties, Durability* (4th ed., pp. 227–316). Springer. https://doi.org/DOI 10.1007/978-3-642-14475-2_5

Ugur, I., Sengun, N., Demirdag, S., & Altindag, R. (2014). Analysis of the alterations in porosity features of some natural stones due to thermal effect. *Ultrasonics*, *54*(5), 1332–1336. https://doi.org/10.1016/j.ultras.2014.01.013

Weiss, T., Rasolofosaon, P. N. J., & Siegesmund, S. (2001). Thermal microcracking in Carrara marble. *Z. Dt. Geol. Ges.*, *152*(2–4), 621–636. https://doi.org/10.1127/zdgg/152/2001/621

Weiss, T., Rasolofosaon, P. N. J., & Siegesmund, S. (2002). Ultrasonic wave velocities as a diagnostic tool for the quality assessment of marble. In Siegfried Siegesmund, T. Weiss, & A. Vollbreecht (Eds.), *Natural*

Stone, Weathering Phenomena, Conservation Strategies and Case Studies (pp. 149–164). The Geological Society of London. https://doi.org/10.1144/GSL.SP.2002.205.01.12

Weiss, T., Siegesmund, S., & Fuller Jr., E. R. (2002). Thermal stresses and microcracking in calcite and dolomite marbles via finite element modelling. In S. Siegesmund, T. Weiss, & A. Vollbrecht (Eds.), *Natural Stone, Weathering Phenomena, Conservation Strategies and Case Studies* (pp. 89–102). The Geological Society of London.

Weiss, T., Siegesmund, S., & Rasolofosaon, P. N. J. (2000). The relationship between deterioration, fabric, velocity and porosity constraint. *The 9th International Congress on Deterioration and Conservation of Stone*, 215–223. https://doi.org/10.1016/B978-044450517-0/50103-3

Widhalm, C., Tschegg, E., & Eppensteiner, W. (1997). Acoustic emission and anisotropic expansion when heating marble. *Journal of Performance of Constructed Facilities*, *11*(1), 35–40. https://doi.org/10.1061/(ASCE)0887-3828(1997)11:1(35)

Yavuz, H., Demirdag, S., & Caran, S. (2010). Thermal effect on the physical properties of carbonate rocks. *International Journal of Rock Mechanics and Mining Sciences*, *47*(1), 94–103. https://doi.org/10.1016/j.ijrmms.2009.09.014

Zeisig, A., Siegesmund, S., & Weiss, T. (2002). Thermal expansion and its control on the durability of marbles. In Siegfried Siegesmund, T. Weiss, & A. Vollbreecht (Eds.), *Natural Stone, Weathering Phenomena, Conservation Strategies and Case Studies* (The Geolog, Vol. 205, pp. 65–80). https://doi.org/10.1144/GSL.SP.2002.205.01.06